Cancer Chemother Pharmacol (2008) 61:377–393
DOI 10.1007/s00280-007-0480-1

ORIGINAL ARTICLE

Glut-1 as a therapeutic target: increased chemoresistance and HIF-1-independent link with cell turnover is revealed through COMPARE analysis and metabolomic studies

Andrew Evans · Victoria Bates · Helen Troy · Stephen Hewitt · Susan Holbeck · Yuen-Li Chung · Roger Phillips · Marion Stubbs · John Griffiths · Rachel Airley

Received: 21 December 2006 / Accepted: 16 March 2007 / Published online: 23 May 2007

Abstract The facilitative glucose transporter Glut-1 is overexpressed and confers poor prognosis in a wide range of solid tumours. The peri-necrotic pattern of expression often seen in human tumour samples is linked with its transcriptional control in hypoxic conditions by hypoxia-inducible factor HIF-1 or through a reduced rate of oxidative phosphorylation. Hypoxia-regulated genes offer promise as novel therapeutic targets as a means of preventing the proliferation and eventual metastatic spread of tissue originating from residual chemically and radio resistant hypoxic cells that have survived treatment. Inhibiting the expression or functionality of Glut-1 may be a way of specifically targeting hypoxic cells within the tumour that depend upon a high rate of glucose uptake for anaerobic glycolysis. We used an array of formalin-fixed, paraffin-embedded samples of the NCI-60 panel of cell lines to carry out immunohistochemical detection of Glut-1 and to select possible candidate lead compounds by COMPARE analysis with agents from the NCI diversity screen, which may work via inhibition of Glut-1 or Glut-1-dependent processes. ''Positive'' COMPARE hits were mostly conjugated *Pseudomonas* toxins binding the epidermal growth factor receptor (EGFR). However, correlations with standard anticancer agents were virtually all negative, indicating a link between Glut-1 and chemoresistance. MTT proliferation assays carried out using stable,

Andrew Evans, Victoria Bates and Helen Troy have contributed equally to this study.

A. Evans · V. Bates · R. Airley
Tumour Metabolism and Therapeutics Group,
School of Pharmacy and Chemistry,
Liverpool John Moores University,
Liverpool L3 3AF, UK
e-mail: a.r.evans@ljmu.ac.uk

V. Bates
e-mail: V.Bates@2004.ljmu.ac.uk

H. Troy · Y.-L. Chung · M. Stubbs · J. Griffiths
CR UK Biomedical Magnetic Resonance Research Group,
Department Basic Medical Sciences,
St George's University of London, London, UK
e-mail: htroy@sgul.ac.uk

Y.-L. Chung
e-mail: ylchung@sgul.ac.uk

M. Stubbs
e-mail: mstubbs@sgul.ac.uk

J. Griffiths
e-mail: jgriffiths@sgul.ac.uk

S. Hewitt
TARP Laboratory, National Cancer Institute,
Bethesda, MD, USA
e-mail: hewitts@mail.nih.gov

S. Holbeck
Developmental Therapeutics Programme,
Information Technology Branch, National Cancer Institute,
Bethesda, MD, USA
e-mail: holbecks@mail.nih.gov

R. Phillips
Tom Connors Cancer Research Centre,
University of Bradford, West Yorkshire, UK
e-mail: r.m.phillips@brad.ac.uk

R. Airley (✉)
Department of Developmental and Molecular Biology,
Chanin Cancer Institute, Albert Einstein College of Medicine,
Bronx, NY, USA
e-mail: rairleyinusa@hotmail.com

Glut-1 overexpressing cell lines generated from the bladder EJ138, human fibrosarcoma HT 1080 and the hepatoma wild type Hepa and HIF-1B-deficient c4 tumour cell lines revealed a cell line-dependent increase in chemoresistance to dacarbazine, vincristine and the bioreductive agent EO9 in Glut-1 overexpressing EJ138 relative to WT and empty vector controls. Metabolomic analysis (^{31}P-MRS and ^{1}H MRS) carried out using cell lysates and xenografts generated from Glut-1 overexpressing Hepa and c4 cell lines showed higher glucose levels in Glut-1 overxpressing c4 relative to parental tumour extracts occurred in the absence of an increase in lactate levels, which were in turn significantly higher in the Glut-1 overexpressing Hepa xenografts. This implies that Glut-1 over-expression without a co-ordinate increase in HIF-1-regulated glycolytic enzymes increases glucose uptake but not the rate of glycolysis. Glut-1 overexpressing xenografts also showed higher levels of phosphodiester (PDE), which relates to the metabolite turnover of phospholipids and is involved in membrane lipid degradation, indicating a mechanism by which Glut-1 may increase cell turnover.

Keywords Glut-1 · HIF-1 · NCI60 · COMPARE analysis · Metabolomics

Introduction

The interest in hypoxia-regulated genes as therapeutic targets in cancer stems from prolific evidence that tumour hypoxia leads to radio and chemoresistance, and that the adaptations afforded by these genes that enable survival in this hostile microenvironment lead to increased malignancy and likelihood of metastatic spread [8, 9, 36]. Tumour hypoxia presents a therapeutic problem; however, the degree of selectivity presented by such microenvironmental differences has provided a number of avenues for exploitation, such as the bioreductive hypoxia-selective cytotoxins. Such agents include tirapazamine, a benzotriazine di-N-oxide currently in phase III clinical trials in non small cell lung and ovarian cancers, which shows particular promise if used in conjunction with radiation therapy or platinum compounds [19]. Another class of bioreductive drugs are the indolequinones, such as E09, which are derivatives of mitomycin C, and are activated by the tumour specific enzyme NQ01 or hypoxia. E09 is currently in Phase I clinical trial for the treatment of bladder cancer [39, 40]. The facilitative glucose transporter Glut-1 is an example of a hypoxia-regulated gene that is overexpressed and confers poor prognosis in a wide range of solid tumours [15, 37]. Glut-1 expression responds to a variety of stimuli. Differences in constitutive Glut-1 expression between tumours and tumour cell lines are likely to be dependent upon factors such as the expression of transforming oncogenes, e.g. H-Ras and c-myc [4, 32]. However, the behaviour of Glut-1 in hypoxic conditions is triphasic, where in acute hypoxia, pre-existing membrane bound protein is demasked or activated, prior to translocation of Glut-1 bound by intracellular vesicles to the plasma membrane. In chronically hypoxic conditions, de novo synthesis occurs, where Glut-1 is dually controlled via the transcription factor HIF-1 and reduced oxidative phosphorylation [54].

The correlation of Glut-1 expression with direct oxygen measurements by Eppendorf histography [1] and via bioreductive marker pimonidazole (Hypoxyprobe®) binding [2] in advanced carcinoma of the cervix suggests that this protein may be used to evaluate the level and extent of hypoxia and hence the suitability of individual patients for hypoxia-dependent therapies such as radiation therapy, as well as for inclusion into clinical trials for hypoxia-selective anticancer agents. The increased uptake and metabolism of glucose in tumours relative to non-malignant tissue was first described by Warburg in 1930, and this effect is most easily explained by the need to support rapidly proliferating tumour tissue, and in hypoxic conditions, a switch to anaerobic glycolysis [55]. These observations have been applied effectively in diagnostic techniques such as FDG-PET [17, 46], as well as therapeutically, where glucose analogues such as 2-deoxyglucose and 5-thioglucose have been used as radiosensitizers or cytotoxic agents which inhibit glucose metabolism [49]. More recent work has evaluated glucose conjugates, where selective uptake of conventional cytotoxic drugs is achieved by conjugation with a glucose moiety. This approach has had a variable degree of success. The agent 2-GluSNAP [11], a glucose-conjugated nitric oxide donor, has shown promise in ovarian carcinoma, whilst the mustard-glucose conjugate gluphosphamide [7], was in phase II clinical trials but showed little clinical advantage and has now been discontinued. The characterisation of Glut-1 and other glucose transporters, together with the rapidly increasing knowledge of the transcriptional pathways involved in oxygen sensing and control of hypoxia-regulated genes is providing the opportunity to investigate the suitability of Glut-1 as a therapeutic target. Whereas previous approaches exploiting glucose metabolism as a target using 2-DG and 5TG were more toxic to hypoxic cells in vitro, this approach was compromised by normal tissue toxicity in mice, presumably due to non-specific inhibition of glycolysis [49]. The importance of Glut-1 in the development of tumours has been explored in vitro and in vivo, where the overexpression of Glut-1 antisense successfully inhibited the proliferation of HL60 leukaemia cells and MKN45-derived xenografts respectively [12, 35]. We have also recently demonstrated that Glut-1 expression may confer resistance to alkylating agents such as dacarbazine, an effect that may be hypoxia independent [3]. Therefore, inhibition of expression or

functionality of Glut-1, rather than inhibiting glucose metabolism in its entirety may more specifically target those cells within the tumour that depend upon a high rate of glucose uptake for anaerobic glycolysis, such as those existing in hypoxic conditions.

The National Cancer Institute Developmental Therapeutics Programme administers a repository of around 140,000 novel, structurally diverse compounds, and has collated toxicity data for an inventory of more than 600,000 standard and novel agents. Toxicity data is derived using sensitivities to the NCI panel of 60 tumour cell lines. The NCI-60 panel of cell lines is now available in the form of an array of formalin-fixed, paraffin-embedded samples of cell lines, enabling rapid and relatively inexpensive detection and racking of molecular target expression by immunohistochemistry and subsequent semi-quantitative grading. In this study, we used this technique to select possible candidate lead compounds by COMPARE analysis using agents from the NCI diversity screen that may work via inhibition of Glut-1 or Glut-1-dependent processes.

Methods

Glut-1 immunohistochemistry

Immunostaining for Glut-1 expression was carried out as described previously [12], according to protocol using Envision kits containing rabbit secondary antibody (DAKO). Primary antibody step for Glut-1 involved incubation for 1 hour at 37°C with a 10 μg/ml concentration of affinity purified anti-rabbit Glut-1 (Alpha Diagnostic International, TX, USA).

Scoring

Glut-1 expression was graded 0–5 according to intensity and spread of staining (0 = no staining, 5 = most intense and widespread Glut-1 staining). Examples of cell lines expressing different grades of Glut-1 expression are shown (Fig. 1).

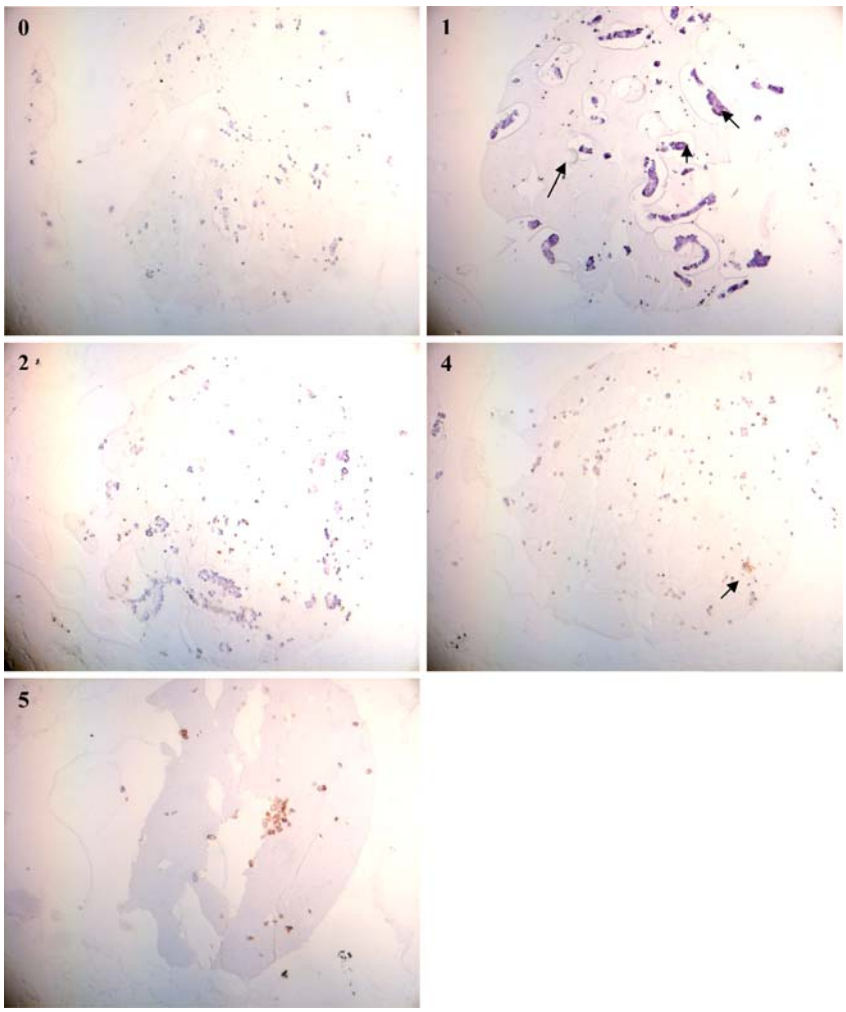

Fig. 1 Scoring was semi-quantitative according to staining distribution and intensity. Examples of Glut- 1 staining intensity scores, including BT549 = 0; MCF7 = 1, OVCAR = 2; IGROV1 = 4; SNB19 = 5, arrow show stained cells. Magnification ×400

COMPARE analysis

A COMPARE analysis was carried out as per Fitzimmons et al. [18] to relate Glut-1 expression in the NCI-60 cell line panel to their sensitivity to standard and novel agents in the NCI drug screen. Using ranked Glut-1 expression as a seed, analysis was carried out as described by the Developmental Therapeutics Programme see website http://www.dtp.nci.nih.gov/docs/compare/compare.html.

Cell culture

Human fibrosarcoma cell lines (HT1080) were obtained from the American Type Culture Collection (Rockville, MD. USA), bladder tumor cell lines kindly donated by Roger Phillips (Bradford, UK) and human hepatoma Hepa wild type and HIF-1-deficient (c4) cell lines were kindly donated by Ian Stratford, Manchester, UK. Cells were maintained at 37°C, 5% CO_2 and 95% humidity in RPMI-1640 medium (Sigma, UK), supplemented with foetal bovine serum (10% v/v) (Invitrogen Ltd., UK).

Preparation of stable cell lines that over-express Glut-1 or Glut-1-GFP fusion protein

Stable cell lines that constitutively overexpress Glut-1 (designated GLAR) were generated as follows. A construct consisting of GLUT-1 cDNA (1,675 bp) (kindly donated by Anthony Carruthers, MA, USA), cloned into the multiple cloning site of pEFIRES-puro plasmid expression vector under the control of a human polypeptide chain elongation factor 1α promoter, was kindly provided by Dr. Kaye Williams (School of Pharmacy and Pharmaceutical Sciences, University of Manchester, UK). Stable transfectants containing either the Glut-1 expression plasmid or empty vector controls were generated using FuGene-6 transfection reagent (Roche Diagnostics Ltd.) according to manufactures instructions, and stable clones selected by culture in medium containing 4 μg/ml puromycin. Glut-1 over-expression from each stable clone was evaluated using immunohistochemistry. The clones showing the highest level of Glut-1 immunostaining plus an empty vector control from each cell line were selected and maintained for a further 4 weeks in medium without selection. Puromycin was then re-introduced for 2 weeks to confirm clone stability. To generate cell lines expressing Glut-1-GFP fusion protein, a GLUT-1 cDNA was inserted into the multiple cloning site of the pEGFP-N3-neo plasmid expression vector (BD Biosciences Clontech, UK) (a gift from Anthony Carruthers, USA). Stable clones expressing the fusion protein were generated from HT1080 cells as per Glut-1 expressing cell lines, using 400 μg/ml G418 (Invitrogen Ltd.) for selection.

Preparation of cells for immunohistochemistry

Exponentially growing cells were harvested into 10 ml ice cold PBS by followed by overnight fixation of pellets with 10% neutral buffered formalin at 4°C. The pellets were carefully submerged in 1% agarose solution, and when set excess agarose was removed before processing through to wax blocks, from which (5 μm) sections were cut and transferred to polylysine coated slides.

Visualisation of expressed Glut-1/EGFP fusion protein

Cells were harvested with trypsin and fixed in neutral buffered formalin (10% (w/v)). The nuclei of the cells were stained with fluorescent Hoechst 33342 (Sigma). The cells were visualised using a BX51 fluorescence microscope (Olympus Optical Co., Japan) at magnification 100× under oil immersion. The Hoechst 33342 stained nuclei of the cells appear blue at a maximum excitation of 340 nm and emission of 488 nm. The EGFP/Glut-1 fusion protein or EGFP appear green at a maximum excitation of 488 nm and emission of 576 nm. Images of the same field of cells were captured separately, at the appropriate wavelengths for Hoechst 33342 or EGFP, using a C4742-95 digital CCD camera (Hamamatsu Phototonics, Japan). These images were merged together using Open Lab™ scientific imaging software (Improvision®, UK).

Western blotting

Over the years we and other groups have experienced many problems with western analysis of Glut-1. Therefore we provide a comprehensive description of the method that worked best for our group, which is based on the immunohistochemistry protocol we have used successfully on many occasions. Cell lysates were prepared by resuspending pellets of freshly harvested (using a cell scraper) exponentially growing cells in ice cold lysis buffer (10 mm Tris–HCl (pH 8), 400 mm NaCl, 100 mM PMSF, 3 mm $MgCl_2$, 1% triton X-100 (v/v), 0.01% (v/v) protease inhibitor cocktail) followed by 30 min incubation on ice to assist lysis. The protein concentration of each sample was determined using the BioRad DC assay. Samples were subjected to deglycosylation using N-glycoidase-F (Sigma) for 24 h at 37°C. After addition of an equal volume of 2× gel loading buffer (500 mM Tris–HCl (pH 6.8), 4.4% (w/v) SDS, 20% (v/v) glycerol, 2% (v/v) β-mercaptoethanol, and 0.04% (w/v) bromophenol blue) to samples containing 20 μg protein, these were boiled for 5 min. Samples were run on 9% SDS-polyacrylamide gels and subsequently transferred to 0.45 μm PVDF membranes. Endogenous peroxidase activity was blocked using buffer containing H_2O_2 (3% for 5 min) and non-specific antibody binding

was inhibited using 1% (v/v) casein solution (Vector Labs) overnight at 4°C. Membranes were then incubated with 2μg/ml affinity purified anti-rabbit Glut-1 antibody (Alpha Diagnostic International, USA) in TBS containing 0.05% (v/v) Tween-20 for 2 h at 37°C. The Envision Kit containing rabbit secondary antibody and DAB liquid substrate (DAKO, UK) was used for chromogenic detection of Glut-1 according to the manufacturer's instructions. Dot blots were generated from 1 μg/μl protein contained in aliquots of 1 μl PBS applied to 0.45μm PVDF membrane and allowed to dry. Subsequent aliquots were cumulatively added as necessary, followed by antibody steps as described above.

Toxicity assays

Cells were seeded at a density of 5×10^4 cells/well in 24-well tissue culture plates and exposed 24 h later to complete medium (control) or increasing doses of drug in complete medium for 24, 48 or 72 h, and MTT proliferation assays carried out as described by Mosmann [34].

Hepa-1 tumour xenograft models

MF-1 nude mice were injected subcutaneously in the flank with a suspension of Hepa-1 cells (10^6) that had been growing as a monolayer in cell culture as described by Griffiths et al. 2002 [21]. Tumour size was calculated by measuring the length, width, and depth of each tumour using callipers and by using the following formula: $lwd(\pi/6)$. A tumour size (approximate volume of 500 mm^3) was used for in vivo MRS experiments.

In vivo ^{31}P-MRS of Hepa-1 tumour xenografts

Tumour-bearing mice were anaesthetized with an intraperitoneal injection of a Hypnovel-Hypnorm-water mixture (1:1:2), positioned in the center of a 12 mm two-turn ^{1}H/^{31}P surface coil and then placed in the bore of a Varian 4.7 Tesla (T) nuclear magnetic resonance (NMR) spectrometer. Image-selected in vivo spectroscopy (ISIS)-localized ^{31}P-MR spectra of the tumours were obtained at 37°C. Briefly, a gradient strength of up to 7.5×10^{-4} T/cm was applied with adiabatic pulses of 500 μs, a 90° sincos excitation pulse, and a 2,000 μs sech 180 inversion pulse, with a total repetition time of 3 s and 600 averages. ^{31}P-MR spectra were quantified using the VARiable PROjection program (VARPRO) to determine precise chemical shifts and peak integrals as previously described [48]. The animals were sacrificed by cervical dislocation and the tumours were removed, freeze-clamped and stored at –80°C for in vitro ^{1}H and ^{31}P-MRS analysis of tumour extracts.

The surface coils used to obtain the ^{31}P-MRS signal from subcutaneous tumours in vivo were of non-uniform spatial sensitivity, so it is not possible to use an internal standard. As a result, the signal intensities observed in the in vivo ^{31}P-MR spectra were expressed as ratios of metabolites.

^{1}H and ^{31}P MRS in vitro

The freeze-clamped tumours were extracted in 6% perchloric acid, as previously described [20]. Neutralized extracts were freeze-dried and reconstituted in 1 ml D_2O, and the extracts (0.5 ml) were placed in 5 mm NMR tubes. ^{1}H MR spectra were obtained using a Bruker 600 MHz spectrometer (pulse angle 45°; repetition time, 3.5 s). The water resonance was suppressed by gated irradiation centred on the water frequency. 25 μl 10 mm Sodium 3-trimethylsilyl-2,2,3,3-tetradeuterpropionate (TSP) was added to the samples for chemical shift calibration and quantification. The pH was re-adjusted to pH 7 prior to ^{1}H MRS.

For ^{31}P MRS, which was carried out after the ^{1}H MRS study, 50 μl 60 mM EDTA was added to each sample for chelation of metals ions, and 25 μl 10 mm methylene diphosphonic acid was added to each sample for chemical shift calibration and quantification. The pH was re-adjusted to pH 7 prior to ^{31}P MRS.

Results

Immunohistochemistry and immunofluorescence studies

Glut-1 staining was frequently cytoplasmic, but in the cell lines showing more intense staining (scores 4 and 5), staining was membranous (Fig. 1).The microarrays allowed reproducible detection and scoring of Glut-1 expression that showed sufficient variation between the NCI60 cell lines to allow ranking in order of staining intensity (Fig. 2). Immunohistochemistry was also used to evaluate the level of Glut-1 expression, which was assigned a (+) value representative of the variation in staining across the range of parental and genetically manipulated cell lines used. There was also a varying differential of staining between normoxic and anoxia-exposed cell lines (Table 1). Glut-1 over expressing cell lines showed increased Glut-1 expression relative to wild type, although the extent of Glut-1 expression also varied amongst the wild type tumor cell lines. Immunofluorescence studies using clones generated to overexpress a Glut-1-GFP fusion protein confirmed the subcellular location of Glut-1, where it was observed in the largest quantities on the plasma membrane,

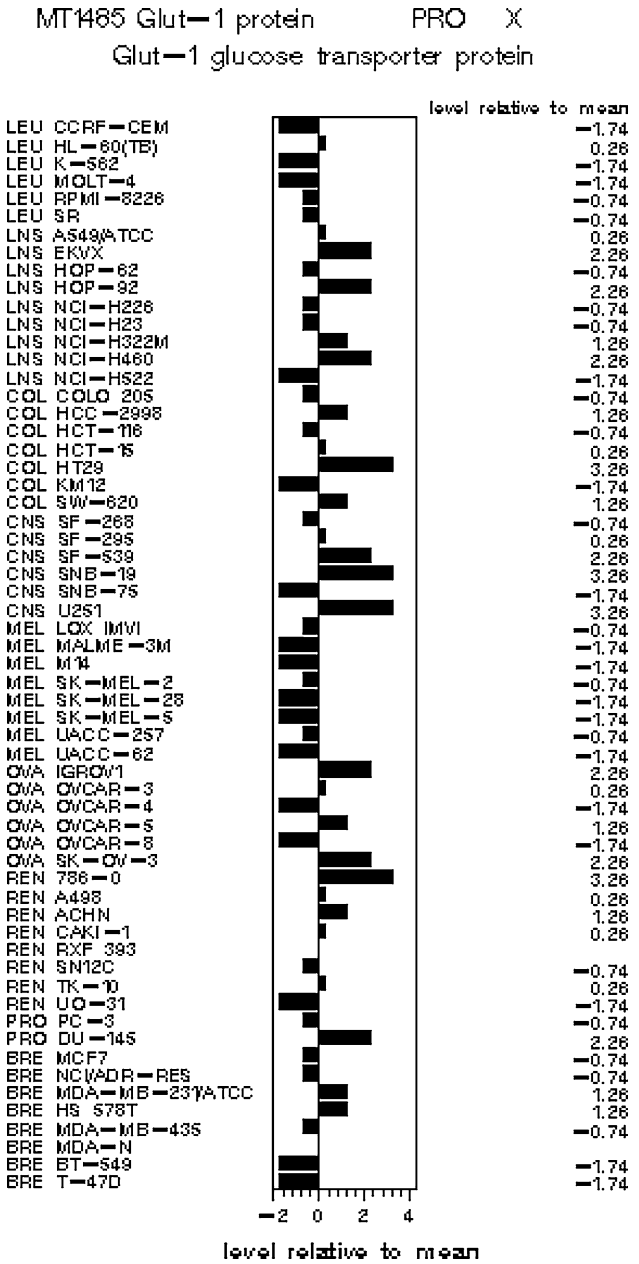

Fig. 2 Glut-1 expression in NCI60 cell lines was scored 0–5 to enable ranking and correlation with toxicity data. The diagram above shows Glut-1 score relative to mean

but also in smaller quantities in the cytoplasm that may have coincided either with intracellular vesicles allowing storage of Glut-1 or with Glut-1 packaging taking place in the golgi apparatus (Fig. 3). The level of Glut-1 protein was also confirmed with immunoblots (Fig. 4). The largest differential of Glut-1 expression was seen between the HIF-1β-deficient mouse hepatoma Hepa-derived c4 cell line and its GLAR clone, as in previous work [53]. Therefore, c4 and their parental Hepa cell lines alongside their respective GLAR clones were used to investigate

Table 1 Glut-1 overexpressing clones, designated GLAR[1], were generated from wild type cell lines transfected with the pEFIRES-puro expression vector containing Glut-1 cDNA or pEFIRES-puro empty vector (controls) using FuGene-6 transfection reagent

Designation	Derivation	Glut-1 xpression[3]	
		Normoxia	Anoxia
HT1080 WT	Human fibrosarcoma	+	+++
HT1080 GLAR[1]		+++++	+++++
HT1080 EV[2]		+	+++
HT29 WT	Human colon carcinoma	+++	+++++
HT29 GLAR		+++++	+++++
HT29 EV		+++	+++++
EJ138 WT	Human bladder carcinoma	+++	++++++
EJ138 GLAR		++++++	ND
EJ138 EV		+++	ND
Hepa-1 WT	Mouse hepatoma	+	+++
Hepa GLAR		+++	+++++
Hepa EV		+	ND
C4 WT	Mouse hepatoma HIF1β-deficient	–	–
C4 GLAR		+++	++++
C4 EV		–	–

[2] EV = empty vector control [3]Glut-1 levels were measured semi-quantitatively using immunohistochemistry in formalin-fixed, paraffin-embedded pellets and dot blots ND = not done. The level of Glut-1 expression was scored using (+) values representative of the variation in staining across the range of parental and genetically manipulated cell lines used. There was also a varying differential of staining between normoxia and anoxia-exposed cell lines

growth kinetics in vivo. The largest differential of Glut-1 expression was between normoxic and anoxic bladder EJ138 wild type cell lines (+++ to ++++++). For this reason, studies of the effect of potential bioreductive agents were focused on this cell line and its respective GLAR clone.

COMPARE analysis

The purpose of this analysis was to determine correlations of Glut-1 protein target data with the mean graph pattern of drug response at the GI50 (50% growth inhibition) level of effect. This included correlations with the (a) standard agents; (b) the BEC-selected agents; (c) molecular target analysis. Statistical significance of Pearson correlations was judged in the context of 30,000 simultaneous comparisons (one for each agent in the database). For this volume of comparisons, a 2-sided P value of 0.05 will lead to on average 30,000/20 = 1,500 false positive conclusions for the case where the target has a true correlation of 0 with all of the agents. In other words, it was expected that all of the top 100 correlates would look extremely significant by

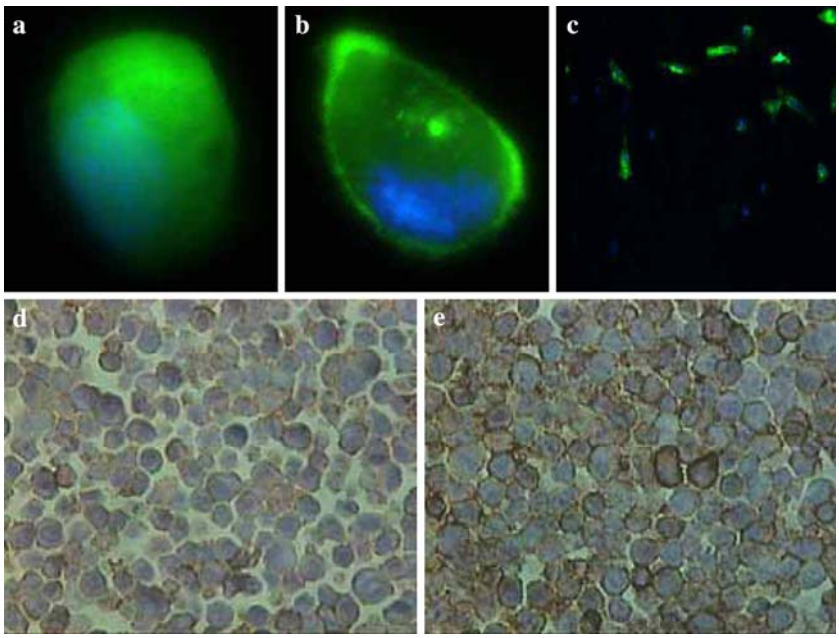

Fig. 3 HT1080 cells were stably transfected to express the fusion protein Glut-1GFP, showing that Glut-1 was mostly targeted to the membrane (b and c) compared to cells transfected to express GFP alone (a) Stable transfectants were also generated to constitutively overexpress Glut-1, panel shows immunohistochemical staining of formalin-fixed, paraffin-embedded cell blocks prepared from (d) wild type fibrosarcoma HT1080; e increased expression of Glut-1 in HT1080-GLAR transfectant

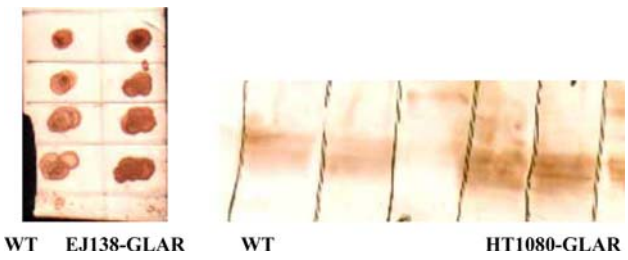

Fig. 4 Dot blot (*left*) and western blot (*right*) showing expression of Glut-1 in stable clones designated GLAR, which were generated to constitutively overexpress Glut-1 relative to wild type (WT)

chance alone. To protect against this, the Bonferroni adjustment was used where only P values less than 0.05/30,000 = 0.000002 (or less than 0.1/30,000 = 0.000003, allowing an experiment-wise false positive rate of 0.1) were treated as statistically significant. This is equivalent to multiplying low P values by 30,000 to assess their true meaning. A positive correlation indicated that a greater abundance of Glut-1 may be associated with sensitivity to the drug, while a negative correlation was indicative of higher levels of Glut-1 conferring cellular resistance to a given drug. Pearson correlation coefficients and two tail P values are shown to help in assigning possible significance to these data. A mechanism of action is assigned to some compounds by a 2 digit code as shown in Fig. 5.

Standard agents

The first 100 rank order correlations were provided, where Pearson correlation coefficients represent the correlation between Glut-1 expression ranked across the NCI-60 cell line panel and the 50% growth inhibitory pattern of response in the NCI-60 cell lines. Details of the drug compounds found in the standard agent database, along with chemical formuli and full details of chemical and biological data are found at http://www.dtp.nci.nih.gov/docs/cancer/searches/standard_agent_table.html. The standard agent database is made up of 170 compounds catalogued by NSC number (the numerical identifier assigned by the NCI developmental therapeutics program), including clinical drugs and agents that failed clinical trial and those in clinical use where a mechanism of action has been defined. Correlations were virtually all inverse, suggesting that Glut-1 was conferring chemoresistance (Fig. 5). Although none of the correlations were statistically significant at the =0.000002 level, it was noteworthy that the alkylating agents dacarbazine (DTIC) and lomustine (CCNU) were ranked at 11th (r = –0.254, P = 0.05) and 18th (r = 0.216, P = 0.103) respectively. The only example of a putative bioreductive agent was mitomycin C, which was ranked 96th and showed no correlation with Glut-1 expression (r = 0.07458, P = 0.57,794). Positive correlations were few and all non-significant, but included vincristine, which was ranked at 26th (r = 0.19816, P = 0.13594).

The BEC-selected database

The first 98 rank ordered correlates are shown against a database of approximately 3,000 open compounds which were selected for evaluation by the Biological Evaluation Committee of Developmental Therapeutics Program. This database has recently been added to the correlative analyses as it contains an enriched group of active compounds

Obs	NSC	CHEMNAME	MOA	Pearson Corr. Coef	P (2- tail)
11	**45388**	**DTIC**		**-0.25425**	**0.05412**
12	143095	PYRAZOFURIN	RO	0.24857	0.05990
13	526417	ECHINOMYCIN		-0.24561	0.06311
14	167780	ASALEY	A7	-0.23928	0.07045
15	349156	PANCRATIASTATIN		-0.23453	0.07639
16	133100	RIFAMYCIN SV		-0.23321	0.07810
17	312887	FLUDARABINE PHOSPHATE		-0.21980	0.09735
18	**79037**	**CCNU**	**AC**	**-0.21606**	**0.10332**
19	192965	SPIROGERMANIUM		-0.21109	0.11170
20	363812	TETRAPLATIN	A7	-0.20867	0.11597
21	102816	5-AZACYTIDINE	RO	-0.20518	0.12234
22	153858	MAYTANSINE	TU	-0.20114	0.13002
23	336628	MERBARONE		-0.20083	0.13062
24	71261	B-TGDR	DI	-0.19966	0.13294
25	21548	THYMIDINE		-0.19835	0.13555
26	**67574**	**VINCRISTINE SULFATE**	**TU**	**0.19816**	**0.13594**
96	26980	MITOMYCIN C	A2	0.07458	0.57794

Fig. 5 Pearson correlation coefficients were calculated to link Glut-1 expression in the NCI60 cell lines with toxicity to drug compounds in the NCI standard agents database. Observed correlations (Obs) are presented in descending order of statistical significance, i.e. according to the numerical (positive or negative) correlation coefficient and *P* value, along with the NSC number (the identifier used by the NCI and the known or proposed mode of action (MOA). For example, observation 11 was the 11th ''strongest'' numerical correlation, but was negative, showing that DTIC (dacarbazine) toxicity across the NCI60 cell line panel correlated to low Glut-1 expression in these cell lines. Although this correlation was weak, and according to the statistical standards as cited by the NCI, it was ''stronger'' than that of the related alkylating agent CCNU, which also correlated negatively with Glut-1 expression but was placed at position 18. Virtually all correlations were inverse, suggesting that high Glut-1 expression induces poor chemoresponse to most agents. The relatively high positions of the alkylating agents dacarbazine (DTIC) and lomustine (CCNU) were redolent of the results of our previous study involving human-tumor-derived xenografts [3]. Modes of action are assigned a two letter code by the DTP as follows: alkylating agents: A2, alkylating at N2 position of guanine; AC, alkyl transferase -dependent cross-linkers; A7, alkylating at N7 position of guanine; anti-DNA agents: DI, incorporated; nucleotide synthesis inhibitors: RO, anti precursors other than folate; TU, tubulin-active antimitotic agents. A list of drug compounds included in the NCI standard agents database, together with their chemical structure and full details of biochemical and chemical data is found at http://www.dtp.nci.nih.gov/docs/cancer/searches/standard_agent_table.html

which helps overcome previous concerns that the overall open database often selects compounds with activity limited to only a few cell lines. A data search for these compounds may be carried out by NSC number at http://www.dtp.nci.nih.gov/dtpstandard/dwindex/index.jsp. All the compounds in the BEC-database have been tested at least twice, and occasional single tests reflect instances where concentration range changes have been made as a result of potency. Again, virtually all correlations were negative. However, there was a short list of positive correlates indicating that Glut-1 expression reflected or conferred chemosensitivity. These consisted mostly of immunotoxins composed of *Pseudomonas* exotoxin A conjugated to cytokines, e.g. TP-38, which targets the epidermal growth factor receptor (Fig. 6), and is currently in phase I and II clinical trials for brain tumours [45].

Molecular target analysis

Molecular target analyses, where included, may indicate possible relationships with other molecular targets in the public domain, or targets where individual contributors have agreed that both parties can be informed of a possible association. Listed associations are those where $P < 0.05$ and (1) pairs of targets with at least one non-binary pattern have been tested for correlation using both Spearman and Pearson test statistics; (2) pairs of binary data targets have been evaluated for associations using the Fishers exact test. In both cases *P*-values were calculated from two-tailed *t* distributions and adjusted using a Bonferroni correction for multiple comparisons as described above (low *P* values multiplied by the number of simultaneous comparisons, to assess their true meaning). Correlations between Glut-1

Obs	NSC		Pearson Corr. Coef	P (2-tail)
15	676498	TP4EK-K6	0.458	3.4E-04
25	671526	Toxin-.delta.53L MW=43000	0.443	5.6E-04
40	623436	TGF alpha-PE40	0.468	1.1E-03
72	676495	TP38-001	0.406	1.7E-03
75	676497	TP4EK	0.404	1.8E-03

Fig. 6 Positive COMPARE hits showed a numerically positive Pearson correlation coefficient. In the BEC database these were mostly conjugated immunotoxins consisting of *Pseudomonas* exotoxin A conjugated to antibodies to transforming growth factor (TGF)

Table 2 Correlations between Glut-1 expression and other molecular targets in the NCI60 cell lines were mostly of low significance, but consisted mainly of tyrosine kinase receptors, with the best correlation being with the colony stimulating factor CSF-1 receptor

PCC	Target	Entity
0.52	TYR kinase CSF1R	RNA
0.52	TYR kinase CSF1R	RNA
0.47	TYR kinase ROR2	RNA
0.46	TYR kinase ROR1	RNA
0.45	TYR kinase EphA7	RNA
0.44	TGF-alpha	RNA

expression and other molecular targets in the NCI60 cell lines were mostly of low significance, but consisted mainly of tyrosine kinase receptors, with the best correlation being with the colony stimulating factor CSF-1 receptor (Table 2).

Glut-1 and chemoresistance to standard agents

MTT proliferation assays were carried out using Glut-1 overexpressing GLAR cell lines in an effort to confirm the hypothesis generating data provided by the COMPARE analysis. Toxicity was calculated as the % reduction in absorbance of treated cells compared to control cells. Firstly, to support the COMPARE analysis and previous work suggesting that Glut-1 conferred resistance to alkylating agents, toxicity to dacarbazine in GLAR clones was determined relative to WT. The effects proved to be cell line dependent, where there was little change in toxicity in Hepa-1/c4 (Fig. 7a) or the HT1080 (Fig. 7b) cell lines. However, when the EJ138 cell lines were treated, the EJ138-GLAR cells were noticeably more resistant (Fig. 7c). The effect of Glut-1 overexpression on this bladder carcinoma cell line was not restricted to dacarbazine, as treatment with the intercalating agent vincristine also revealed a similar Glut-1-mediated chemoresistance (Fig. 8), an effect that held after 72 h drug exposure. MTT assays were also carried out using EJ138 empty vector controls, and their sensitivity to dacarbazine was similar to that of wild type cells (data not shown).

Positive COMPARE ''Hits''

To more accurately determine if Glut-1 conferred sensitivity to the immunotoxins, TP-38 was kindly donated by the Pastan laboratory (Laboratory of Molecular Biology, Center for Cancer Research, National Cancer Institute, National Institute of Health). Data from MTT assays carried out using HT1080-GLAR versus WT (Fig. 9a) show no observable difference in chemosensitivity. Early work

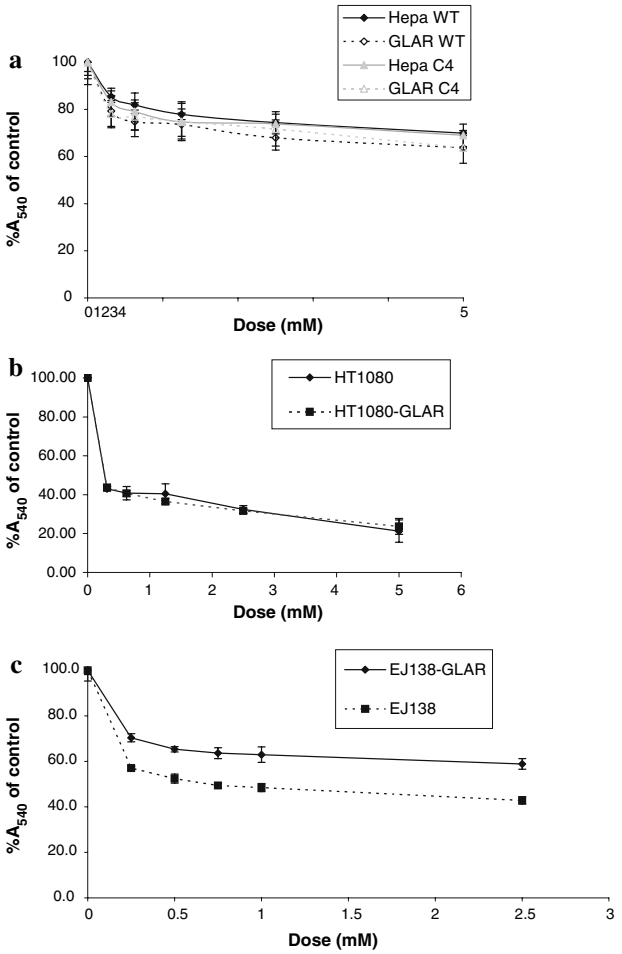

Fig. 7 MTT proliferation assays were carried out to assess chemosensitivity to dacarbazine (presented as percentage absorbance of untreated controls), showing that overexpression of Glut-1 had little effect on dacarbazine toxicity in the Hepa-1 and HIF-1B-deficient c4 (**a**) or the human fibrosarcoma HT1080 cell lines after 48 h drug exposures in normoxic conditions (**b**). However, Glut-1 overexpression apparently effected a decrease in dacarbazine toxicity (48 h exposures) in the bladder carcinoma cell line EJ138 (c), showing that Glut-1-mediated chemoresistance may be cell line-dependent

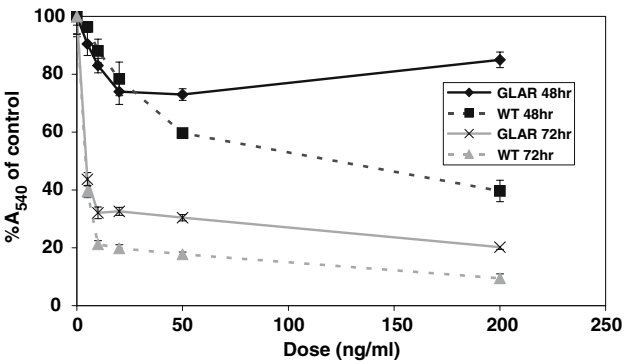

Fig. 8 MTT assays revealed that EJ138-GLAR cells were less sensitive to vincristine relative to wild type, after 48 and 72 h drug exposures

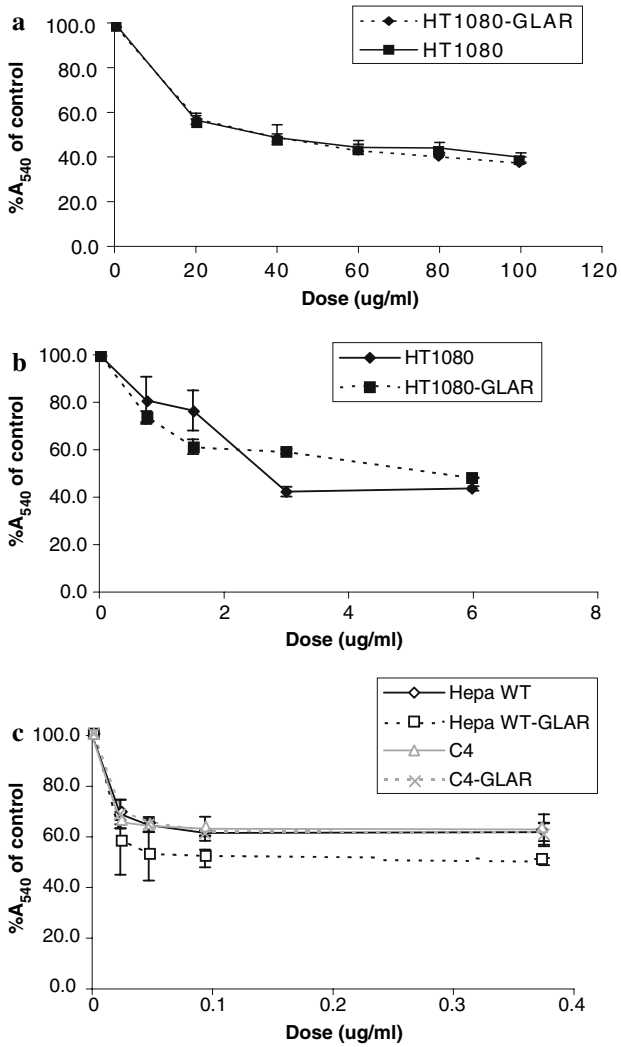

Fig. 9 HT1080-GLAR versus wild type was exposed to the EGF-binding *Pseudomonas* toxin TP-38 for 72 h. Overexpression of Glut-1 caused no observable difference in sensitivity to TP-38 relative to wild type cells (**a**). To rule out the possibility that sensitivity to the conjugated immunotoxins was due to the effects of the *Pseudomonas* exotoxin alone, HT1080-GLAR (**b**) and HEPA-1/C4-GLAR (**c**) and respective wild type cell lines were treated with unconjugated *Pseudomonas* exotoxin A. Apart from a slight increase in sensitivity in the Hepa-GLAR cell lines, overexpression of Glut-1 appeared to have no clear effect, despite very early reports that the mechanism of exotoxin-mediated toxicity is through increased glucose uptake

showed that *Pseudomonas* exotoxin toxicity to mammalian cells is modified in the presence of 2-deoxyglucose, suggesting that the toxicity of bacterial exotoxins is glucose-dependent, possibly by a mechanism that relates to the internalization of the toxin Deem et al. [16]. To rule out the possibility that the COMPARE data may be due to the effect of the *Pseudomonas* exotoxin rather than the TGFα antibody conjugate, toxicity assay were carried out using *Pseudomonas* exotoxin (Sigma) alone in HT1080-GLAR (Fig. 9b) and Hepa-1/c4-GLAR (Fig. 9c) relative to wild type cells. Apart from a slight increase in sensitivity in the Hepa-GLAR cell lines, overexpression of Glut-1 appeared to have no clear effect.

Influence of Glut-1 on chemoresistance to bioreductive agents

Glut-1 has been used as a surrogate marker of hypoxia by virtue of its regulation by HIF-1 and its link with an increased rate of anaerobic and aerobic glycolysis in malignant tissue. Bioreductive agents may to differing degrees be preferentially activated in hypoxic conditions, as long as there are sufficient tumor associated enzymes to catalyse this reaction. One such bioreductive agent, EO9, is an indoloquinone anticancer drug (3-hydroxy-5-aziridinyl-1-2-(1H-indole-4,7-dione)prop-β-enα-ol), which is related to the bioreductive alkylating agent mitomycin C but is less myelosuppressive [23]. Activation of this drug is in the form of a 2-electron reduction catalysed by the tumour-associated reductase NQ01. The influence of hypoxia on the cytotoxicity of this drug is contentious, as in pre-clinical studies, cell lines with high levels of DTD show little, if any increase in sensitivity under hypoxic conditions, whereas cell lines with low levels of DTD show a marked increase in sensitivity [41]. Under aerobic conditions, cells containing the highest levels of DTD tended to show the greatest sensitivity to EO9 [42]. By virtue of promising preclinical data in bladder carcinoma cell lines, E09 is currently in phase II trials for the treatment of transitional cell bladder carcinomas [51]. It is possible that Glut-1 expression may correlate with EO9 cytotoxicity either independently or as a reflection of its ability to predict hypoxia. Therefore MTT assays were carried out to compare sensitivity of Glut-1 overexpressing bladder EJ138 cells to wild type in normoxic or anoxic conditions. There appears to be a clear hypoxic differential in this cell line, where both GLAR and wild type cells were more sensitive to E09 in anoxic conditions. However, Glut-1 overexpression still appears to confer increased chemoresistance in both normoxic and anoxic conditions (Fig. 10).

Growth characteristics of Glut-1 overexpressing xenografts

Immunohistochemistry carried out on xenograft material showed that the relative level of Glut-1 protein expressed in tumours derived from genetically manipulated cell lines was similar to that occurring in vitro (Fig. 11). Growth characteristics of Hepa-1-derived tumor xenograft models were similar to previously published data from Williams et al. [53], where there was an initial growth delay in the HIF-1B-deficient c4-derived xenografts compared with growth of HEPA-1 WT tumors. Generation of Glut-1

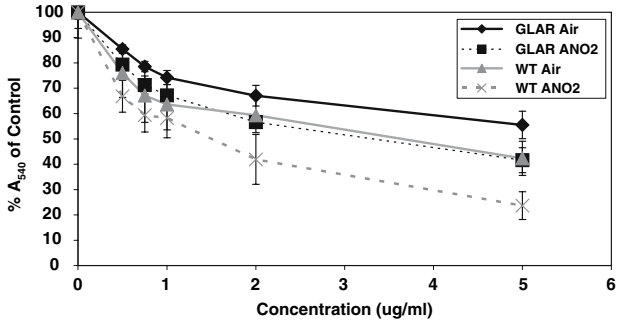

Fig. 10 To determine whether Glut-1 expression might influence sensitivity to bioreductive agents, MTT assays were carried out after exposure to E09. Overexpression of Glut-1 decreased sensitivity of bladder EJ138 cells to E09 in normoxia and anoxia. There appears to be a clear hypoxic differential in this cell line, where both GLAR and wild type cells were more sensitive to E09 in anoxic conditions. However, these experiments suggest that Glut-1 overexpression still appears to confer increased chemoresistance independently of hypoxia

overexpressing Hepa-1 and c4-derived xenografts enabled us to reintroduce Glut-1 back into HIF-1-deficient tumors and so observe the influence of Glut-1 on tumor growth independently of other HIF-1-regulated genes. Accordingly, there was a non-significant trend of faster growth in the c4-GLAR relative to the parental c4-derived xenografts, to a growth rate approaching that of the Hepa-WT xenografts. Here, final tumor volumes at day 23 were 499 ± 51 mg for the c4 compared to 595 ± 85 mg for the c4-GLAR-derived xenografts. However, when it came to xenografts showing a complete HIF-1 response, Hepa-GLAR-derived xenografts seemed to have a slower rate of growth than those of the wild type Hepa-1, reaching final tumor volumes before sacrifice of 466 ± 118 mg and 697 ± mg respectively (Fig. 12).

Metabolomics of Hepa-1-derived xenografts

Metabolomic profiling was carried out to confirm the functionality of the GLAR clones with regard to the downstream effects of increased glucose transport on tumor metabolism, where data is shown in Table 3.

In vivo ^{31}P-MRS

No differences were found comparing the Hepa-1 WT with Hepa-GLAR tumours. The phosphodiester (PDE) peak was larger in the c4-GLAR tumours compared with those generated from Hepa-GLAR cells. PDE/TP and PDE/βNTP ratios were significantly higher in the c4-GLAR relative to Hepa-GLAR tumours, whereas PME/PDE ratio was significantly lower in the c4-GLAR tumours.

In vitro ^{1}H-MRS

The c4-GLAR tumour extracts showed higher ($P < 0.006$) glucose compared to c4-parental but no statistically significant difference in lactate. The c4-GLAR tumour extracts also had a statistically significantly higher ($P < 0.005$) phosphocholine (PC) content, which is involved in membrane lipid synthesis. Comparing the Hepa-GLAR with the c4-GLAR tumours, glucose levels were higher in the c4-GLAR tumor extracts; although lactate levels were higher in the Hepa-GLAR tumour extracts. As reported previously [20], glycine, betaine and PC were lower in the c4-parental relative to the Hepa-1 WT—derived tumor extracts. We also found that the c4-derived tumours had lower glucose and lactate levels relative to Hepa-1 WT

In vitro ^{31}P-MRS

No difference was seen between the Hepa-GLAR and Hepa-1 WT tumours, although PC was higher in c4-GLAR compared with c4 parental tumours. This is in agreement with the ^{1}H-MRS result. Lower PC levels were found in tumours derived from Hepa-1 WT parental relative to c4 cells, where these results are in agreement with previously published data by Griffiths et al. [21].

Discussion

The interest in Glut-1 as a therapeutic target stems from both the proliferation of studies in human tumour samples that show its adverse effect on prognosis, and from its role as a hypoxia-regulated gene under the control of HIF-1. The use of HIF-1-regulated genes as targets for novel anticancer strategies still has momentum, but this is mostly confined to the development of therapies targeted against HIF-1 via their action on upstream or downstream targets in the HIF pathway. For example, the agent YC-1, via its action on soluble guanyl cyclase, and the thioredoxin-1 (Trx-1) inhibitors PX-1 and PX-478 both reduce HIF-1 transactivation activity in vitro and in xenografts. In vivo studies suggest that the timing, but not the extent, of HIF-1 activity during the development and growth of a tumor is critical. A study carried out in HIF-1α null xenografts showed that HIF-1, by virtue of its ability to confer an adaptive response in the developing tumour, has a positive effect on tumour growth [43]. Xenografts generated from HIF-1-deficient mouse hepatoma cells, however, showed a rate of growth similar to wild type tumours, although a lag phase after implantation was observed [29]. The effect of HIF-1 activity upon growth of xenografts also appears to have little relationship with the percentage of HIF-1

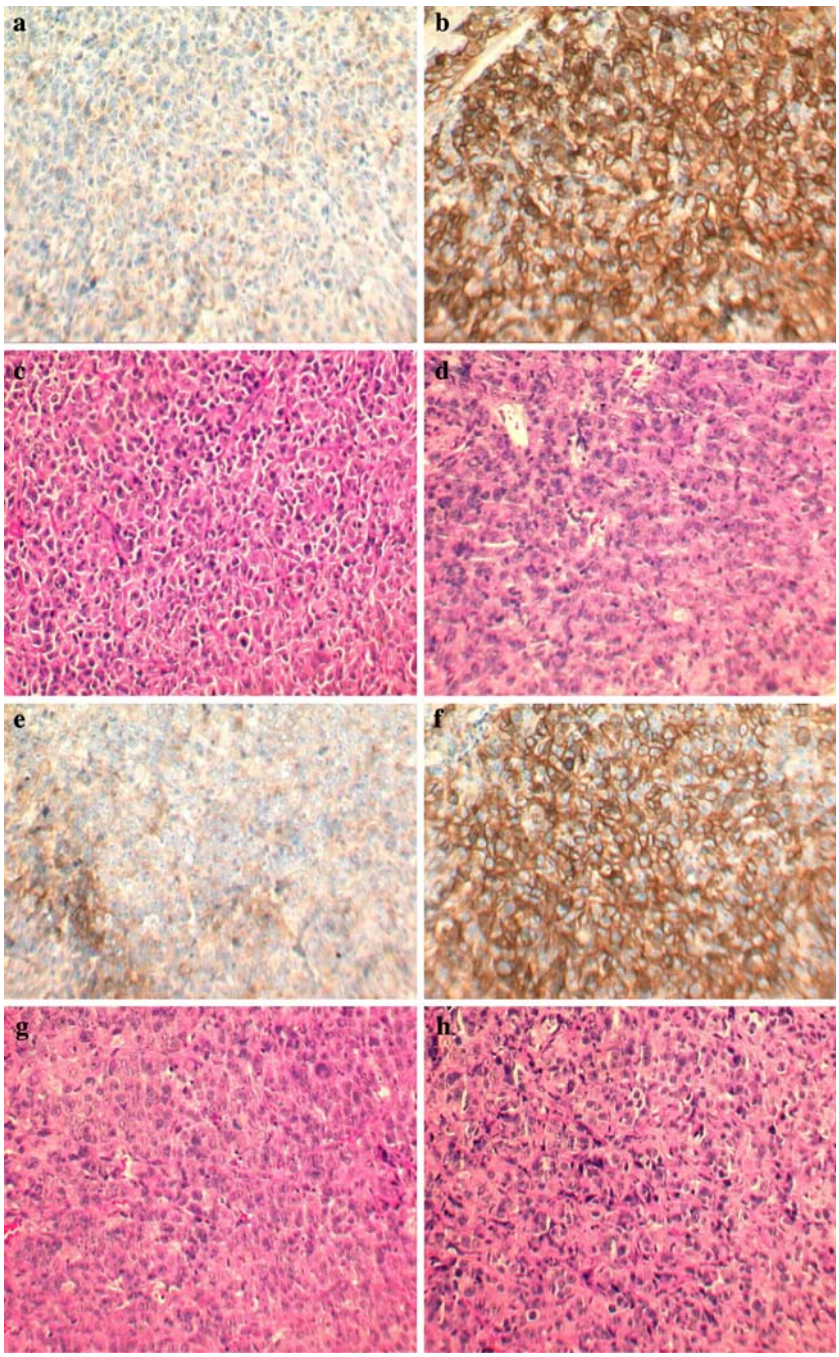

Fig. 11 Glut-1 immunohistochemistry of xenograft material. Glut-1 expression was maintained when xenografts were generated from GLAR clones, and was homogeneously expressed in both HIF-1B-deficient c4-GLAR (**b**) and Hepa-GLAR (**f**)-derived tumors. This was in contrast to xenografts derived from wild type Hepa cell lines, where the classical peri-necrotic pattern of staining was observed (**e**), and negligible amounts of Glut-1 was detected in c4-dereived xenografts (**a**). H and E staining showed morphology and architecture of the tumors were not compromised. **c** c4; **d** c4-GLAR; **g** Hepa WT; **h** Hepa-GLAR. × 20

expressing cells, where cell mixing experiments have revealed that a few cells with a complete HIF-1 response is adequate to sustain the growth of a whole tumor Hopfl et al. [24]. This has important implications for the use of HIF-1 as a target, as a complete eradication of HIF-1 expressing cells may need to be carried out to obtain a chemoresponse. Nevertheless, the drive to develop HIF-1-targeted therapies is often diverted to the inhibition of angiogenesis, and is based upon blockade of growth factors such as vascular endothelial growth factor (VEGF), EGF and their respective tyrosine kinase type receptors VEGFR and EGFR (reviewed by Harris [22]). A study involving the generation of dominant negative HIF-1 expressing xenografts suggests that the tumorigenic effects of HIF-1 are via an effect upon glucose metabolism [13], but does not examine the effect of downregulated HIF-1-regulated genes such as carbonic anhydrase IX [20] or monocarboxylate transporter MCT4 [50], which may influence the handling of lactate. The value of this present study is therefore to help determine the merit of Glut-1 as a

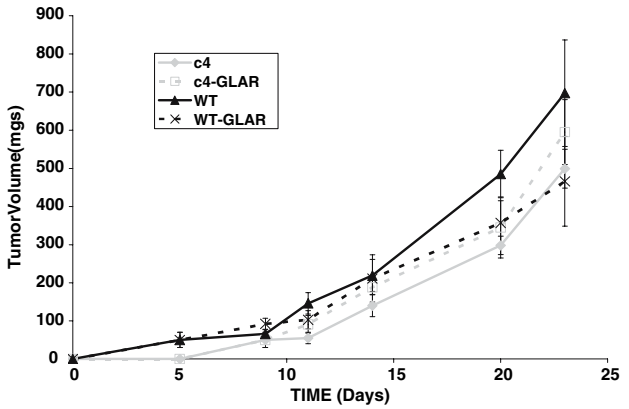

Fig. 12 Growth characteristics of Hepa-1-derived tumor xenograft models. The initial lag phase seen in HIF-1B-deficient xenografts shown previously was maintained even in Glut-1 overexpressing cell lines. However, growth rate of c4-GLAR xenografts was increased relative the c4 parental line, where Glut-1 overexpression may be compensating for the effects of an absent HIF-1 response

therapeutic target, not only as a major survival signal downstream of HIF-1, but as a target separate and distinct from the other HIF-1 regulated genes.

The COMPARE analysis has provided strong evidence that Glut-1 is an indicator of chemoresistance, where the role of Glut-1 was successfully validated in toxicity studies using Glut-1 overexpressing cell lines. Disappointingly, the COMPARE analysis and the subsequent toxicity assays yielded no statistically significant data that could be used to identify lead drug compounds. However, the positive correlation between Glut-1 expression and the EGFR-binding immunotoxins is interesting, and in the absence of data confirming the Glut-1-dependent cytotoxicity, this correlation may be a reflection of a biological association between Glut-1, EGFR and HIF-1, where both EGFR and Glut-1 are targets of HIF-1, and EGF may stimulate Glut-1 expression [6, 25].

It is arguably more difficult to design drugs that inhibit a channel protein than it is for an enzyme or a membrane bound receptor. The effort to design drugs targeting p-glycoprotein, a transmembrane carrier protein that shares some of the structural characteristics of Glut-1, creates a precedent, however, for example the results of phase I trials of the p-glycoprotein inhibitor Ontogen were recently published [14]. There has been significant progress in the theoretical and experimental characterisation of Glut-1 crystal structure, which may prove useful as start points for the rational design of Glut-1 inhibiting agents. In particular, homology modelling studies carried out by the Fischbarg laboratory have enabled construction of a three-dimensional model of Glut-1 [44] that exhibits the topological and biochemical features compiled in part through extensive work carried out alongside the Carruthers and Golde groups. Cumulatively, this work identifies possible sites of inhibition for a putative Glut-1 targeting agent. Glut-1 is a nucleotide-binding protein, presenting two ATP-binding cassettes which are critical for the conformation and therefore transporter affinity. When ATP is in position within its domains, glucose is occluded within a post-translocation vestibule formed by Glut1 cytosolic domains [29, 30]. The mechanism is pH dependent, and one can also speculate that this is the mechanism by which reduced ATP levels and the consequent ‘‘opening’’ of Glut-1 to glucose leads to the demasking or activation of Glut-1 in acutely hypoxic conditions [5]. Thus, it is possible that a pharmacological strategy to effect Glut-1 blockade would be via the ATP-binding site- in fact it has been shown that isoflavone ATP-binding tyrosine kinase inhibitors such as genestein and quercetin are able to bind and inhibit Glut-1 by this mechanism [52]. In view of these findings, we are currently investigating the role of Glut-1 in the action of the clinically used ATP-binding tyrosine kinase imatinib and gefitinib in Glut-1 overexpressing xenografts.

The high level of Glut-1 expression in the blood-brain barrier helps maintain basal glucose levels in the brain, which would be a major therapeutic problem to overcome if Glut-1 were to be targeted. The effect of Glut-1 blockade may be predicted by considering patients with Glut-1-deficiency syndrome, an autosomal dominant trait that varies in severity with genotype and age. Two classes of mutation have been described as the molecular basis for the functional defect of glucose transport: hemizygosity of GLUT1 and nonsense mutations resulting in truncation of the GLUT-1 protein [47]. Glut-1 deficiency syndrome, or De Vivo syndrome, is characterised by infantile seizures, developmental delay, acquired microcephaly, spasticity, ataxia, and hypoglycorrhachia. Clinical signs show lower than normal levels of glucose and consequently lactate in the cerebrospinal fluid, but glucose uptake by erythrocytes, which also express large quantities of Glut-1, may or may not be affected [28]. Interestingly, despite the obvious risk of morbidity, the patients have responded well to a ketogenic diet, where protein is used as an alternative energy source to the brain [27]. Therefore, a major adverse effect that may be associated with non-specific blood-brain barrier Glut-1 blockade arising from the targeting of tumour Glut-1 is seizures at the time or following treatment, although lessons learnt from the treatment of patients with Glut-1 deficiency may offer a way of overcoming such adverse effects if tumour response to such agents warrants it. The development of Glut-1 inhibiting agents would also need to include monitoring of cerebrospinal fluid glucose and lactate levels as pre-clinical studies. Studies investigating the use of glucose analogues or glucose conjugates that are likely to be taken up into target cells through

Table 3 Metabolomic analysis was carried out in vivo (31P MRS), where signal intensities were expressed as ratios of metabolites

Metabolites	Hepa-GLAR	c4-GLAR	Hepa-1 WT	c4
^{31}P MRS (in vivo)				
NTP/TP	0.62 ± 0.03	0.54 ± 0.01	0.56 ± 0.03	0.62 ± 0.01 [b]
PDE/TP	0.05 ± 0.01	0.11 ± 0.01[a]	0.06 ± 0.02	0.07 ± 0.01
PDE/βNTP	0.26 ± 0.01	0.64 ± 0.06[a]	0.36 ± 0.11	0.37 ± 0.06
PME/PDE	3.75 ± 0.59	1.65 ± 0.21[a]	4.58 ± 2.10	2.61 ± 0.64
^{1}H MRS (tissue extracts)				
Lactate	8.62 ± 1.50	3.33 ± 0.67[a]	5.62 ± 0.65	3.62 ± 0.33 [b]
Alanine	2.84 ± 0.32	1.00 ± 0.09 [a]	1.85 ± 0.32 [c]	1.60 ± 0.39 [d]
Choline	0.31 ± 0.09	0.24 ± 0.06	0.25 ± 0.02	0.33 ± 0.02 [b]
PC	1.56 ± 0.35	1.91 ± 0.09	1.49 ± 0.19	0.98 ± 0.13[b,d]
GPC	0.61 ± 0.19	1.28 ± 0.24	0.70 ± 0.07	1.49 ± 0.16 [b]
Betaine	0.50 ± 0.14	0.14 ± 0.09	0.64 ± 0.34	0.18 ± 0.04 [b]
Glycine	1.79 ± 0.32	1.02 ± 0.09	1.63 ± 0.12	1.13 ± 0.15 [b]
Glucose	0.22 ± 0.06	1.25 ± 0.24 [a]	0.36 ± 0.05	0.21 ± 0.05 [b, d]
^{31}P MRS (tissue extracts)				
PC	0.92 ± 0.31	1.13 ± 0.06	0.89 ± 0.10	0.48 ± 0.04 [b, c]
GPE	0.14 ± 0.05	0.38 ± 0.05	0.16 ± 0.04	0.35 ± 0.05 [b]
GPC	0.47 ± 0.17	0.81 ± 0.12[a]	0.25 ± 0.03	0.73 ± 0.06 [b]

Data is expressed as Mean + SEM. using a two-tailed *t* test for significance. Statistical significance values are $P < 0.05$

[a] Significant difference comparing Hepa-GLAR with c4-GLAR

[b] Significant difference comparing c4-GLAR with c4 parental

Metabolites were measured in vitro by 1H MRS of the tissue extracts. Data is expressed as μmol/g wet weight. Mean + SEM. A two-tailed *t* test with $P < 0.05$ for significance levels was used

[a] Significant difference comparing Hepa-GLAR with c4-GLAR

[b] Significant difference comparing Hepa-1 WT with c4

[c] Significant difference comparing Hepa-GLAR with Hepa-1

[d] Significant difference comparing c4-GLAR with c4-derived xenograft extracts

Metabolite levels were also measured in tissue *ts* by 31P MRS. Data expressed as μmol/g wet weight. Mean + SEM. A two-tailed *t* test with $P < 0.05$ for significance levels was used

[a] Significant difference comparing Hepa-GLAR with c4-GLAR

[b] Significant difference comparing Hepa-1 WT with c4

[c] Comparing c4-GLAR with c4-derived xenograft extracts

Glut-1, offer compelling evidence that the differential of Glut-1 expression between the brain and tumors is large enough to allow targeting of Glut-1. For instance, the PET tracer FDG has recently been investigated in mouse models of breast cancer as a radiomolecular therapy, and doses up to 5 mCi proved to be non-radiotoxic to normal organs [33].

The metabolomic characterisation of the Glut-1 over-expressing xenografts contributes to the understanding of the role of HIF-1 in tumours. It is clear from the growth rate of c4-GLAR-derived xenografts that Glut-1 is an important part of the positive effect of HIF-1 on tumour growth. However, the higher glucose levels in c4-GLAR relative to c4-parental tumour extracts occurs without an increase in lactate levels, which are significantly higher in the HEPA-GLAR xenografts. This implies that Glut-1 over-expression without a co-ordinate increase in HIF-1-regulated glycolytic enzymes increases glucose uptake but not the rate of glycolysis. Increased Glut-1 expression may have an effect on mechanisms of cellular proliferation that are independent of HIF-1. To support this hypothesis, further experiments are required to examine if this apparent effect holds after recovery of the complete HIF-1 response. For this purpose, we are currently carrying out experiments using Hepa-derived cell lines that have undergone an identical mutagenic response to the c4 cells, but that have been allowed to revert back to a state where they show normal HIF-1β expression [53]. To fully evaluate the interaction between Glut-1-associated chemorestance and the intact HIF-1 response, there are now in existence a range of cell lines showing absence of either HIF-1α or β. For instance, xenografts generated using the HIF-1α-deficient Chinese hamster ovary cell line

show similar growth kinetics relative to wild type as the Hepa-c4-derived xenografts [53]. Cells that overexpress a dominant negative version of HIF-1α have also been used to determine the influence of HIF-1 in malignant progression, hypoxia marker expression, glucose metabolism and chemoresistance [10, 13, 26] and introduction of Glut-1 into these cell lines as a means of addressing the need for intact HIF-1 to induce Glut-1-mediated chemoresistance may also be possible. A further strategy currently in progress is to generate and evaluate chemoresistance in tumour cell lines that have downregulated, via RNA interference, Glut-1 expression. Interestingly, cardiomyocytes undergoing such treatment showed reduced HIF-1α expression [31]. Therefore, reintroduction of HIF-1α into a similarly treated Glut-1-downregulated tumour cell line could also help to distinguish Glut-1 and HIF-1-mediated effects on proliferation and chemoresistance. In the present work, Glut-1 was not measured at the mRNA level. Analysis of protein is arguably more straightforward and less expensive than RNA-based techniques when using formalin-fixed biopsy material to evaluate potential markers of treatment sensitivity in a clinical setting. However, analysis of Glut-1 at the mRNA level in future work may provide more data on the molecular signalling pathways occurring, particularly in hypoxic conditions, which determine the relative influence of Glut-1 and HIF-1 on chemoresponse. Another interesting outcome of the study is the finding that Glut-1 overexpressing xenografts have higher levels of PDE. This relates to the metabolite turnover of phospholipids and is involved in membrane lipid degradation, so reveals a mechanism by which Glut-1 may increase cell turnover. In generating Glut-1 overexpressing cell lines and xenografts that have proven to be metabolically functional, we now have a model with which to test putative Glut-1 inhibitors. Applying this model to the use of hypoxia-targeted therapy, although there appeared to be endogenous Glut-1 staining in the parental c4-derived xenografts, it is unlikely that this was related to hypoxic induction as it bore little resemblance to the membranous, peri-necrotic pattern of Glut-1 staining typically observed in tumor hypoxia [1, 2, 15]. This endogenous Glut-1 expression may be explained by fluctuation of microenvironmental glucose levels, or through signalling by oncogenes known to induce Glut-1 expression [38]. Therefore, the existence of endogenous Glut-1 staining is unlikely to be of consequence in the use of Glut-1 overexpressing xenografts**.** The study offers further evidence that Glut-1 confers chemoresistance in both standard and bioreductive agents. For bioreductive agents, meanwhile, the hypoxia may cause opposing effects on chemoresponse, both inducing the expression of Glut-1, and causing chemical activation of the prodrug. In view of this, prospective studies, where Glut-1 is used to select patients to receive bioreductive agents or more aggressive chemotherapy will be useful.

References

1. Airley R, Loncaster J, Davidson S, Bromley M, Roberts S, Patterson A, Hunter R, Stratford I, West C (2001) Glucose transporter glut-1 expression correlates with tumor hypoxia and predicts metastasis-free survival in advanced carcinoma of the cervix. Clin Cancer Res 7:928–934
2. Airley RE, Loncaster J, Raleigh JA, Harris AL, Davidson SE, Hunter RD, West CM, Stratford IJ (2003) GLUT-1 and CAIX as intrinsic markers of hypoxia in carcinoma of the cervix: relationship to pimonidazole binding. Int J Cancer 104:85–91
3. Airley RE, Phillips RM, Evans AE, Double J, Burger AM, Feibig HH, West CM, Stratford IJ (2005) Hypoxia-regulated glucose transporter Glut-1 may influence chemosensitivity to some alkylating agents: results of EORTC (First Translational Award) study of the relevance of tumour hypoxia to the outcome of chemotherapy in human tumour-derived xenografts. Int J Oncol 26:1477–1484
4. Baron-Delage S, Mahraoui L, Cadoret A, Veissiere D, Taillemite JL, Chastre E, Gespach C, Zweibaum A, Capeau J, Brot-Laroche E, Cherqui G (1996) Deregulation of hexose transporter expression in Caco-2 cells by ras and polyoma middle T oncogenes. Am J Physiol 270: G314–G323
5. Behrooz A, Ismail-Beigi F (1999) Stimulation of glucose transport by hypoxia: signals and mechanisms. News Physiol Sci 14:105–110
6. Bos R, van Diest PJ, de Jong JS, van der Groep P, van der Valk P, van der Wall E (2005) Hypoxia-inducible factor-1alpha is associated with angiogenesis, and expression of bFGF, PDGF-BB, and EGFR in invasive breast cancer. Histopathology 46:31–36
7. Briasoulis E, Judson I, Pavlidis N, Beale P, Wanders J, Groot Y, Veerman G, Schuessler M, Niebch G, Siamopoulos K, Tzamakou E, Rammou D, Wolf L, Walker R, Hanauske A (2000) Phase I trial of 6-hour infusion of glufosfamide, a new alkylating agent with potentially enhanced selectivity for tumors that overexpress transmembrane glucose transporters: a study of the European Organization for Research and Treatment of Cancer Early Clinical Studies Group. J Clin Oncol 18:3535–3544
8. Brizel DM, Sibley GS, Prosnitz LR, Scher RL, Dewhirst MW (1997) Tumor hypoxia adversely affects the prognosis of carcinoma of the head and neck. Int J Radiat Oncol Biol Phys 38:285–289
9. Brown JM (2002) Tumor microenvironment and the response to anticancer therapy. Cancer Biol Ther 1:453–458
10. Brown LM, Cowen RL, Debray C, Eustace A, Erler JT, Sheppard FC, Parker CA, Stratford IJ, Williams KJ (2006) Reversing hypoxic cell chemoresistance in vitro using genetic and small molecule approaches targeting hypoxia inducible factor-1. Mol Pharmacol 69:411–418
11. Cantuaria G, Magalhaes A, Angioli R, Mendez L, Mirhashemi R, Wang J, Wang P, Penalver M, Averette H, Braunschweiger P (2000) Antitumor activity of a novel glyco-nitric oxide conjugate in ovarian carcinoma. Cancer 88:381–388
12. Chan JY, Kong SK, Choy YM, Lee CY, Fung KP (1999) Inhibition of glucose transporter gene expression by antisense nucleic acids in HL-60 leukemia cells. Life Sci 65:63–70
13. Chen J, Zhao S, Nakada K, Kuge Y, Tamaki N, Okada F, Wang J, Shindo M, Higashino F, Takeda K, Asaka M, Katoh H, Sugiyama T, Hosokawa M, Kobayashi M (2003) Dominant-negative hypoxia-inducible factor-1 alpha reduces tumorigenicity of pancreatic cancer cells through the suppression of glucose metabolism. Am J Pathol 162:1283–1291

14. Chi KN, Chia SK, Dixon R, Newman MJ, Wacher VJ, Sikic B, Gelmon KA (2005) A phase I pharmacokinetic study of the P-glycoprotein inhibitor, ONT-093, in combination with paclitaxel in patients with advanced cancer. Invest New Drugs 23:311–315
15. Cooper R, Sarioglu S, Sokmen S, Fuzun M, Kupelioglu A, Valentine H, Gorken IB, Airley R, West C (2003) Glucose transporter-1 (GLUT-1): a potential marker of prognosis in rectal carcinoma?. Br J Cancer 89:870–876
16. Deem RL, Niederlehner A, Targan SR (1986) Active target cell processes, possibly involving receptor-mediated endocytosis, are critical for expression of cytotoxicity by natural killer cell-derived cytolytic factor. Cell Immunol 102:187–197
17. Eubank WB, Mankoff DA (2005) Evolving role of positron emission tomography in breast cancer imaging. Semin Nucl Med 35:84–99
18. Fitzsimmons SA, Workman P, Grever M, Paull K, Camalier R, Lewis AD (1996) Reductase enzyme expression across the National Cancer Institute Tumor cell line panel: correlation with sensitivity to mitomycin C and EO9. J Natl Cancer Inst 88:259–269
19. Gandara DR, Lara PN Jr, Goldberg Z, Le QT, Mack PC, Lau DH, Gumerlock PH (2002) Tirapazamine: prototype for a novel class of therapeutic agents targeting tumor hypoxia. Semin Oncol 29:102–109
20. Grabmaier K, MC AdW, Verhaegh GW, Schalken JA, Oosterwijk E (2004) Strict regulation of CAIX(G250/MN) by HIF-1alpha in clear cell renal cell carcinoma. Oncogene 23:5624–5631
21. Griffiths JR, McSheehy PM, Robinson SP, Troy H, Chung YL, Leek RD, Williams KJ, Stratford IJ, Harris AL, Stubbs M (2002) Metabolic changes detected by in vivo magnetic resonance studies of HEPA-1 wild-type tumors and tumors deficient in hypoxia-inducible factor-1beta (HIF-1beta): evidence of an anabolic role for the HIF-1 pathway. Cancer Res 62:688–695
22. Harris AL (2002) Hypoxia—a key regulatory factor in tumour growth. Nat Rev Cancer 2:38–47
23. Hendriks HR, Pizao PE, Berger DP, Kooistra KL, Bibby MC, Boven E, Dreef-van der Meulen HC, Henrar RE, Fiebig HH, Double JA et al (1993) EO9: a novel bioreductive alkylating indoloquinone with preferential solid tumour activity and lack of bone marrow toxicity in preclinical models. Eur J Cancer 29A:897–906
24. Hopfl G, Wenger RH, Ziegler U, Stallmach T, Gardelle O, Achermann R, Wergin M, Kaser-Hotz B, Saunders HM, Williams KJ, Stratford IJ, Gassmann M, Desbaillets I (2002) Rescue of hypoxia-inducible factor-1alpha-deficient tumor growth by wild-type cells is independent of vascular endothelial growth factor. Cancer Res 62:2962–2970
25. Ishida K, Yamashita H, Katagiri H, Oka Y (1995) Regulation of glucose transporter 1 (GLUT1) gene expression by epidermal growth factor in bovine corneal endothelial cells. Jpn J Ophthalmol 39:225–232
26. Jensen RL, Ragel BT, Whang K, Gillespie D (2006) Inhibition of hypoxia inducible factor-1alpha (HIF-1alpha) decreases vascular endothelial growth factor (VEGF) secretion and tumor growth in malignant gliomas. J Neurooncol 78:233–247
27. Klepper J, Scheffer H, Leiendecker B, Gertsen E, Binder S, Leferink M, Hertzberg C, Nake A, Voit T, Willemsen MA (2005) Seizure control and acceptance of the ketogenic diet in GLUT1 deficiency syndrome: a 2- to 5-year follow-up of 15 children enrolled prospectively. Neuropediatrics 36:302–308
28. Klepper J, Voit T (2002) Facilitated glucose transporter protein type 1 (GLUT1) deficiency syndrome: impaired glucose transport into brain– a review. Eur J Pediatr 161:295–304
29. Levine KB, Cloherty EK, Hamill S, Carruthers A (2002) Molecular determinants of sugar transport regulation by ATP. Biochemistry 41:12629–12638
30. Liu Q, Vera JC, Peng H, Golde DW (2001) The predicted ATP-binding domains in the hexose transporter GLUT1 critically affect transporter activity. Biochemistry 40:7874–7881
31. Malhotra R, Tyson DG, Sone H, Aoki K, Kumagai AK, Brosius FC 3rd (2002) Glucose uptake and adenoviral mediated GLUT1 infection decrease hypoxia-induced HIF-1alpha levels in cardiac myocytes. J Mol Cell Cardiol 34:1063–1073
32. Merrall NW, Plevin R, Gould GW (1993) Growth factors, mitogens, oncogenes and the regulation of glucose transport. Cell Signal 5:667–675
33. Moadel RM, Nguyen AV, Lin EY, Lu P, Mani J, Blaufox MD, Pollard JW, Dadachova E (2003) Positron emission tomography agent 2-deoxy-2-[18F]fluoro-D-glucose has a therapeutic potential in breast cancer. Breast Cancer Res 5:R199–R205
34. Mosmann T (1983) Rapid colorimetric assay for cellular growth and survival: application to proliferation and cytotoxicity assays. J Immunol Methods 65:55–63
35. Noguchi Y, Saito A, Miyagi Y, Yamanaka S, Marat D, Doi C, Yoshikawa T, Tsuburaya A, Ito T, Satoh S (2000) Suppression of facilitative glucose transporter 1 mRNA can suppress tumor growth. Cancer Lett 154:175–182
36. Nordsmark M, Bentzen SM, Rudat V, Brizel D, Lartigau E, Stadler P, Becker A, Adam M, Molls M, Dunst J, Terris DJ, Overgaard J (2005) Prognostic value of tumor oxygenation in 397 head and neck tumors after primary radiation therapy. An international multi-center study. Radiother Oncol 77:18–24
37. Oliver RJ, Woodwards RT, Sloan P, Thakker NS, Stratford IJ, Airley RE (2004) Prognostic value of facilitative glucose transporter Glut-1 in oral squamous cell carcinomas treated by surgical resection; results of EORTC Translational Research Fund studies. Eur J Cancer 40:503–507
38. Osthus RC, Shim H, Kim S, Li Q, Reddy R, Mukherjee M, Xu Y, Wonsey D, Lee LA, Dang CV (2000) Deregulation of glucose transporter 1 and glycolytic gene expression by c-Myc. J Biol Chem 275:21797–21800
39. Phillips RM (1998) Prospects for bioreductive drug development. Expert Opin Investig Drugs 7:905–928
40. Phillips RM, Jaffar M, Maitland DJ, Loadman PM, Shnyder SD, Steans G, Cooper PA, Race A, Patterson AV, Stratford IJ (2004) Pharmacological and biological evaluation of a series of substituted 1,4-naphthoquinone bioreductive drugs. Biochem Pharmacol 68:2107–2116
41. Plumb JA, Gerritsen M, Milroy R, Thomson P, Workman P (1994) Relative importance of DT-diaphorase and hypoxia in the bioactivation of EO9 by human lung tumor cell lines. Int J Radiat Oncol Biol Phys 29:295–299
42. Robertson N, Haigh A, Adams GE, Stratford IJ (1994) Factors affecting sensitivity to EO9 in rodent and human tumour cells in vitro: DT-diaphorase activity and hypoxia. Eur J Cancer 30A:1013–1019
43. Ryan HE, Poloni M, McNulty W, Elson D, Gassmann M, Arbeit JM, Johnson RS (2000) Hypoxia-inducible factor-1alpha is a positive factor in solid tumor growth. Cancer Res 60:4010–4015
44. Salas-Burgos A, Iserovich P, Zuniga F, Vera JC, Fischbarg J (2004) Predicting the three-dimensional structure of the human facilitative glucose transporter glut1 by a novel evolutionary homology strategy: insights on the molecular mechanism of substrate migration, and binding sites for glucose and inhibitory molecules. Biophys J 87:2990–2999
45. Sampson JH, Akabani G, Archer GE, Bigner DD, Berger MS, Friedman AH, Friedman HS, Herndon JE 2nd, Kunwar S, Marcus S, McLendon RE, Paolino A, Penne K, Provenzale J, Quinn J, Reardon DA, Rich J, Stenzel T, Tourt-Uhlig S, Wikstrand C, Wong T, Williams R, Yuan F, Zalutsky MR, Pastan I (2003) Progress report of a Phase I study of the intracerebral microinfusion of a recombinant chimeric protein composed of

transforming growth factor (TGF)-alpha and a mutated form of the Pseudomonas exotoxin termed PE-38 (TP-38) for the treatment of malignant brain tumors. J Neurooncol 65:27–35
46. Schwartz DL, Rajendran J, Yueh B, Coltrera MD, Leblanc M, Eary J, Krohn K (2004) FDG-PET prediction of head and neck squamous cell cancer outcomes. Arch Otolaryngol Head Neck Surg 130:1361–1367
47. Seidner G, Alvarez MG, Yeh JI, O'Driscoll KR, Klepper J, Stump TS, Wang D, Spinner NB, Birnbaum MJ, De Vivo DC (1998) GLUT-1 deficiency syndrome caused by haploinsufficiency of the blood-brain barrier hexose carrier. Nat Genet 18:188–1891
48. Stubbs M, Van den Boogaart A, Bashford CL, Miranda PM, Rodrigues LM, Howe FA, Griffiths JR (1996) 31P-magnetic resonance spectroscopy studies of nucleated and non-nucleated erythrocytes; time domain data analysis (VARPRO) incorporating prior knowledge can give information on the binding of ADP. Biochim Biophys Acta 1291:143–148
49. Tannock IF, Guttman P, Rauth AM (1983) Failure of 2-deoxy-D-glucose and 5-thio-D-glucose to kill hypoxic cells of two murine tumors. Cancer Res 43:980–983
50. Ullah MS, Davies AJ, Halestrap AP (2006) The plasma membrane lactate transporter MCT4, but not MCT1, is up-regulated by hypoxia through a HIF-1alpha-dependent mechanism. J Biol Chem 281:9030–9037
51. van der Heijden AG, Moonen PM, Cornel EB, Vergunst H, de Reijke TM, van Boven E, Barten EJ, Puri R, van Kalken CK, Witjes JA (2006) Phase II marker lesion study with intravesical instillation of apaziquone for superficial bladder cancer: toxicity and marker response. J Urol 176:1349–53; discussion 1353
52. Vera JC, Reyes AM, Velasquez FV, Rivas CI, Zhang RH, Strobel P, Slebe JC, Nunez-Alarcon J, Golde DW (2001) Direct inhibition of the hexose transporter GLUT1 by tyrosine kinase inhibitors. Biochemistry 40:777–790
53. Williams KJ, Telfer BA, Airley RE, Peters HP, Sheridan MR, van der Kogel AJ, Harris AL, Stratford IJ (2002) A protective role for HIF-1 in response to redox manipulation and glucose deprivation: implications for tumorigenesis. Oncogene 21:282–290
54. Zhang JZ, Behrooz A, Ismail-Beigi F (1999) Regulation of glucose transport by hypoxia. Am J Kidney Dis 34:189–202
55. Zu XL, Guppy M (2004) Cancer metabolism: facts, fantasy, and fiction. Biochem Biophys Res Commun 313:459–465